



Original Article

Stress Distribution and Displacement of Craniofacial Structures Following Rapid Maxillary Expansion in Different Types of Cleft Palate: A Three-Dimensional FEM Study

Esra Bölükbaşı¹, Berza Yılmaz², Sabri İlhan Ramoğlu³

¹Specialist in Orthodontics, Private Practice, İstanbul, Turkey

²Department of Orthodontics, Faculty of Dentistry, Bezmialem Vakıf University, İstanbul, Turkey

³Department of Orthodontics, Faculty of Dentistry, Altınbaş University, İstanbul, Turkey

Cite this article as: Bölükbaşı E, Yılmaz B, İlhan Ramoğlu S. Stress distribution and displacement of craniofacial structures following rapid maxillary expansion in different types of cleft palate: A three-dimensional fem study. *Turk J Orthod.* 2021; 34(2): 77-85.

Main Points

- Different types of clefts demonstrated different patterns of stress distribution.
- The highest stress accumulation was observed in the isolated cleft model.
- The level of stress distributed at the cleft side was greater than that at the non-cleft side.
- The maximum transversal expansion was observed in the bilateral cleft model.

ABSTRACT

Objective: To evaluate displacements and stress distributions in finite element models (FEMs) of the craniofacial complex of 13-year-old male patient with complete unilateral cleft palate (UCP), a 15-year-old female patient with complete bilateral cleft palate (BCP), and a 15-year-old female patient with isolated cleft palate (ICP), which may respond differently to expansive forces.

Methods: The FEMs were based on computed tomography scans of patients with UCP, BCP, and ICP who needed maxillary expansion. Von Mises stress distribution after 0.2 mm of expansion and displacements after 5 mm of expansion were investigated.

Results: The highest amount of stress was observed in the ICP model. Surprisingly, no stress was noted around the nose in the BCP model. The amount of dentoalveolar expansion decreased from anterior to posterior on the cleft side of the UCP, BCP, and ICP models. In contrast, on the non-cleft side of the UCP model, the maximum dentoalveolar expansion occurred at the molar area, decreasing toward the anterior parts. Anatomical structures expressed posterior displacement in the UCP model. In the ICP model, structures close to midline showed anterior displacement, while structures in the lateral parts showed posterior displacement. In contrast with the other 2 models, the structures in the BCP model showed anterior displacement. Vertically, all the anatomic structures in the BCP model showed inferior displacement, while in the ICP and UCP models, only the structures close to the midline showed inferior displacement.

Conclusion: Maxillary expansion caused different patterns of stress distribution and displacement in different types of clefts. Clinicians should consider the type of the cleft, and may expect differing patterns of widening following maxillary expansion.

Keywords: Unilateral, bilateral, isolated, cleft palate, rapid maxillary expansion, finite element method

INTRODUCTION

Cleft lip and palate (CLP) is one of the most common congenital anomalies affecting the facial structure, characterized by underdeveloped maxilla in the transverse, sagittal, and vertical planes.¹ Both environmental and genetic factors are involved in their formation. This condition requires a meticulous multidisciplinary approach for dental treatments and orthognathic rehabilitation.²

It is common to see a maxillary transverse deficiency, constricted upper arch, and crossbite in patients with CLP, related to underdeveloped maxilla and scar tissue contractions following repair surgeries.³ Even though the necessity of long-term retention because of the tendency to relapse are mentioned in the literature, rapid maxillary expansion (RME) is often applied to correct the transverse discrepancies in CLP patients.³

The finite element method (FEM) is a helpful mathematical tool to use in dentistry, in which the shape of complex geometric objects and their physical properties are simulated digitally. The greatest advantage of this method is the ability to predict changes in areas where measurement is not possible in living individuals. However, the FEM results are highly dependent on the quality of the constructed models. Therefore, the models must be developed to approximate the real object as closely as possible in various aspects. Increasing the number of elements used in the FEM increases the accuracy of the results.^{4,5}

Many studies in the literature examined the effects of RME in patients without a cleft. It has been documented in clinical and finite element analysis studies that circummaxillary and craniofacial structures are affected with and displaced by this orthopedically effective procedure.^{5,6} The effects of the RME vary depending on the design of the expansion appliances, the supporting structures, and the resistance of the anatomical structures depending on the age of the patients.⁴ However, there is no study on the changes related to RME in patients with different cleft types, in whom the outcomes of this procedure might have particularly crucial importance due to lack of integrity of the surrounding anatomic units.

This study aimed to evaluate the patterns of displacement and stress distribution in the craniofacial complex using an RME appliance in 3 models with different types of CLP—bilateral, unilateral, and isolated cleft palate—by using finite element analysis (FEA).

METHODS

3D finite element models (FEMs) were generated using data extracted from archived dental volumetric tomography (DVT) scan images of a 13-year old male patient with complete unilateral cleft palate (UCP), a 15-year-old female patient with complete bilateral cleft palate (BCP), and a 15-year-old female patient with isolated cleft palate (ICP) (isolated cleft of the secondary palate) with institutional review board approval. In addition, the bilateral cleft patient had posterior bilateral crossbite, the unilateral cleft patient had anterior crossbite, and the isolated cleft patient had posterior bilateral crossbite. All the patients previously signed an informed consent form stating that their archive data could be used for scientific purpose.

CT scan images recorded with 5-mm intervals were taken in the axial direction while the Frankfort plane was parallel to the horizontal plane. The Digital Imaging and Communications in Medicine (DICOM) data of the DVT scan was imported using

Mimics software (Version 10.01; Materialize, Leuven, Belgium), the bone tissue was calibrated, and models containing only the nasomaxillary complex and the cranial bones were obtained by subtracting the mandibular and vertebral parts from the whole cranium. The models' surfaces were smoothed by clearing the sharp bone margins or filling the bone defects using Geomagic Design X (Rock Hill, SC, USA).

Solid models were created using SOLIDWORKS 2016 software (SOLIDWORKS Corp, Waltham, MA, USA) and, geometric points along the detectable centerline of the facial bones were defined and assigned X, Y, and Z coordinates, which were fed into the preprocessor of the software for grid generation. An expansion appliance containing a Hyrax screw (Leone, Florence, Italy) was modeled and positioned parallel to the midpalatal suture, as close to the palate as possible (Figure 1). ANSYS Version 17.0 (Canonsburg, PA, USA) was used for the FEA. In addition, a zero-displacement and rotation boundary condition was defined on the nodes along with the foramen magnum. This study was approved by the ethics committee of the clinical researches (03.06.2015-11/16), and DVTs used in the study were selected from previous images taken for clinical orthodontic treatment.

The bone volumes were meshed with 10-node tetrahedral elements. The UCP model consisted of approximately 1 799 565 tetrahedral elements and 2 785 413 nodes, the BCP model consisted of approximately 1 609 498 elements and 2 508 593 nodes. The ICP model consisted of approximately 2 117 163 tetrahedral elements and 3 198 386 nodes (Figure 2).

The material properties were assigned to the various structures, referring to previous studies (Table 1).⁷⁻⁹ Materials in the analysis were assumed to be linearly elastic, isotropic, and homogeneous.

Zero-displacement and rotation boundary conditions were defined on the nodes around the foramen magnum, and all the displacements were restricted to this area. Von Mises stress

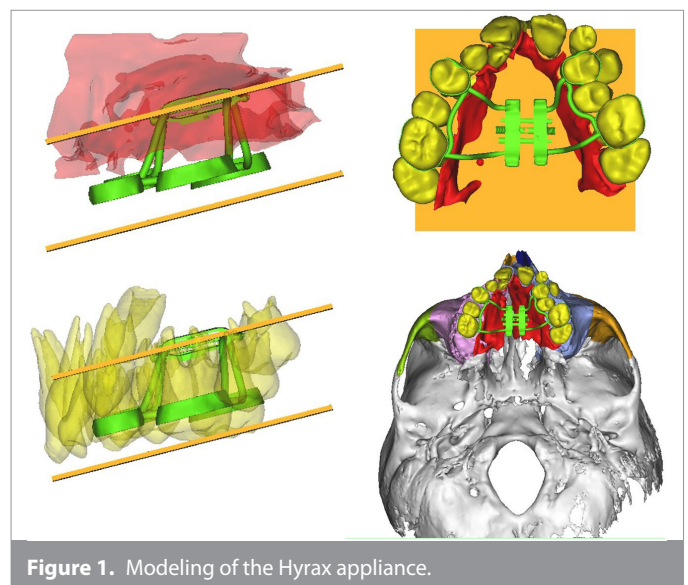


Figure 1. Modeling of the Hyrax appliance.

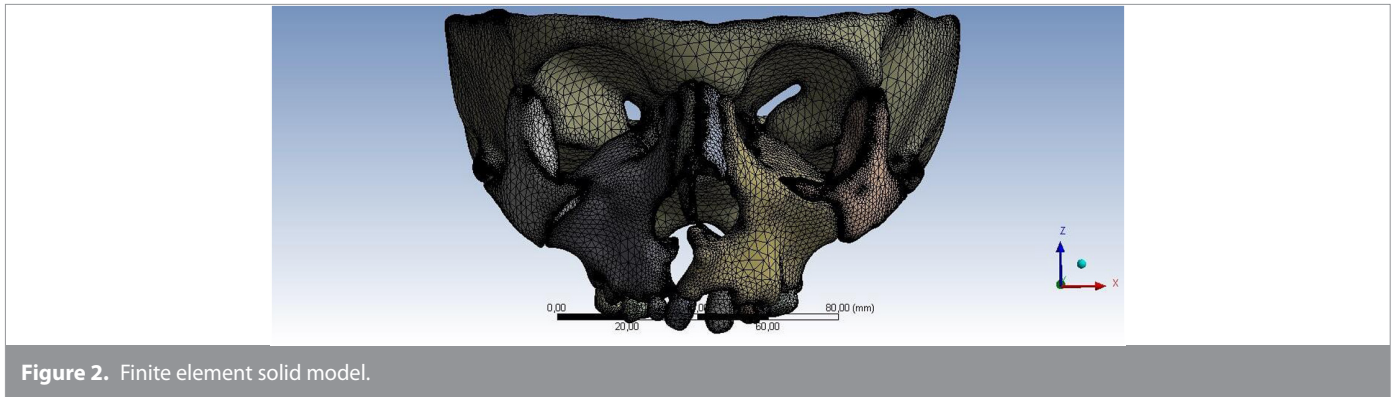


Figure 2. Finite element solid model.

distribution was evaluated following 0.25 mm of screw opening, and displacements resulting from 5 mm of expansion were analyzed.

RESULTS

Displacements

The 3D coordinates were recorded for various craniofacial structures before and after the screw activation in all 3 dimensions (x, transverse plane; y, sagittal plane; and z, vertical plane). Displacements of the anatomic units following 5 mm of screw opening in different types of cleft models are given in Table 2. Mean displacements were calculated for the bilateral and isolated cleft palate (CP). Positive changes indicated outward, backward, and downward displacements (Figure 3A-C, Table 2).

In the UCP model, the anatomic units showed more displacement at the cleft side than those located at the non-cleft side, indicating that expansion forces do not have symmetric outcomes. The maximum lateral displacement on the non-cleft side for maxillary teeth was observed at the molar area. On the other hand, the amount of displacements on the cleft side tended to decrease along the canine region toward the posterior segment. The amount of antero-posterior displacements in the cleft and non-cleft sides were once again uneven, but in general, structures in both cleft and non-cleft sides displaced posteriorly. The nasomaxillary complex opened in a triangular shape with the base downwards as expected. In the vertical plane, the structures close to the midline, such as the internasal, frontonasal, frontomaxillary, and nasomaxillary sutures, displaced downward. On the other hand, the structures located more laterally, such as zygomaticotemporal or zygomaticomaxillary sutures, showed upward displacement.

Table 1. Properties of materials used in the finite element model analysis

	Young's modulus (MPa)	Poisson's ratio
Compact bone	13 700	0.3
Cancellous bone	1370	0.3
Suture	10	0.49
Tooth	20 290	0.3
PDL	0.68	0.49
Stainless steel	210 000	0.3

In the BCP model, dental units showed a marked amount of displacement in the transverse plane. The amount of displacement tended to decrease along the canine region toward the posterior segment. The anterior displacement of the dentoalveolar units was decreasing toward the posterior part. The internasal and frontonasal suture regions showed no displacement in the transverse, anteroposterior, and vertical planes. All other anatomic structures showed a tendency to displace inferiorly.

In the ICP model, the expansion resulted in a wedge-shaped opening in the transverse plane. The lateral displacement of the anterior structures was greater than the lateral displacement of the posterior structures. Similarly, inferior structures showed more lateral displacement than superior structures. In the Y-axis, structures close to the midline showed anterior displacement (frontonasal suture, ANS, apical region of incisors, apical region of canine), while structures in the lateral parts showed posterior displacement. In the vertical plane, structures close to the midline showed inferior displacement, while the lateral structures tended toward superior displacement.

von Mises Stress Distributions

The von Mises stress distributions following 0.2 mm of screw opening in different CP models are given in Table 3. In the unilateral cleft model, the maximum von Mises stress accumulation was observed on the internasal, frontomaxillary, zygomaticomaxillary suture landmarks, and the inferior orbital rim on the cleft side. The level of stress distributed at the cleft side was greater than that at the non-cleft side. In the BCP model, the highest stress was observed in the zygomaticomaxillary suture area. In the ICP model, the highest stress was observed in the internasal suture followed by nasomaxillary suture. The highest stress accumulation in the dentoalveolar area was observed in the molar regions (Figure 4A-C and Table 3).

DISCUSSION

The FEM proves to be an important instrument in the medical field and in orthodontic research, since it permits us to highlight the stress distribution areas and the displacement of anatomic units in a non-invasive and replicable manner. With FEM, it is possible to anticipate the tissue responses to mechanical forces by dividing complex structures into smaller sections with adjustable elastic properties. The control of the simplification degree represents the great advantages of this method. On the

Table 2. Displacement pattern of different cleft palate patients

	Unilateral cleft palate				Bilateral cleft palate				Isolated cleft palate						
	u_x (mm)		u_y (mm)		u_x (mm)		u_y (mm)		u_x (mm)		u_y (mm)		u_z (mm)		
	Cleft side	Non-cleft side	Cleft side	Non-cleft side	Cleft side	Non-cleft side	Cleft side	Non-cleft side	Cleft side	Non-cleft side	Cleft side	Non-cleft side	Cleft side	Non-cleft side	
Sutura internasalis	0.12	0.12	0.12	0.12	-0.3	-0.3	0	0	0	0	0.14	0.17	0.14	0.17	-0.26
Sutura frontonasalis	0.19	0.18	0	0.12	-0.12	-0.34	0	0	0	0	0.01	-0.08	0.01	-0.08	-0.17
Sutura frontomaxillaris	0.08	0	0	0.2	-0.12	-0.33	0.06	-0.03	-0.56	0	0	0.11	0.11	0	-0.37
Sutura nasomaxillaris	-0.12	0	0.05	0.22	-0.21	-0.36	0.16	-0.08	-0.54	0	0.11	0.16	0.11	0.16	-0.38
Sutura frontozygomatica	-0.03	0.01	0.23	0.06	0.34	0.12	-0.49	0	0	-0.06	0.05	0.05	-0.06	0.05	0.06
Sutura temporozygomatica	-0.19	0.43	0.28	-0.03	0.39	0.19	-0.5	0	0	-0.18	0.18	0.18	-0.18	0.18	0.22
Sutura zygomaticomaxillaris	-0.69	0.48	0.26	0.02	-0.86	0.01	-0.67	-0.06	-0.1	-0.34	0.14	0.14	-0.34	0.14	0.06
Infraorbital margin	-0.33	0.27	0.19	0.09	0.32	-0.06	-0.67	-0.08	-0.08	-0.27	0.11	0.11	-0.27	0.11	-0.02
Foramen infraorbitalis	-0.6	0.41	0.16	0.13	0.45	-0.08	-0.71	-0.17	-0.32	-0.35	0.09	0.09	-0.35	0.09	-0.09
Zygomatic process	-1.06	0.66	0.19	0	0.63	-0.1	-0.9	-0.03	-0.23	-0.52	0.15	0.15	-0.52	0.15	-0.02
Lateral nasal wall	-0.81	0.34	0.04	0.2	-0.04	-0.3	-0.82	-0.31	-0.49	-0.52	0.05	0.05	-0.52	0.05	-0.37
ANS	-	0.43	-	0.26	-	-0.44	-	-	-	-1.16	-0.05	-0.05	-1.16	-0.05	-0.8
Point A	-	0.52	-	0.25	-	-0.48	-	-	-	-0.95	0	0	-0.95	0	-0.59
Apical region of incisors	-	0.56	-	0.17	-	-0.37	-	-	-	-1.05	-0.08	-0.08	-1.05	-0.08	-0.61
Apical region of canine	-1.38	0.63	0	0.05	0.27	-0.21	-1.16	-0.23	-0.54	-1	-0.08	-0.08	-1	-0.08	-0.33
Apical region of premolars	-1.19	0.68	0.14	0.01	0.54	-0.17	-1.14	-0.07	-0.38	-0.83	0.14	0.14	-0.83	0.14	-0.14
Apical region of molars	-1.08	0.71	0.16	-0.01	0.56	-0.15	-1	0.01	-0.31	-0.65	0.17	0.17	-0.65	0.17	-0.02
Retromolar region	-0.88	0.74	0.16	0	0.47	-0.18	-0.93	-0.08	-0.46	-0.4	0.14	0.14	-0.4	0.14	-0.02
Tip of the upper central incisor	-	0.81	-	0.11	-	-0.38	-	-	-	-1.38	-0.1	-0.1	-1.38	-0.1	-0.6
Tip of the upper canine	-1.79	0.82	-0.1	0.07	-0.11	-0.33	-1.51	-0.2	-0.53	-1.27	-0.07	-0.07	-1.27	-0.07	-0.4
Tip of the upper premolar	-1.66	0.88	-0.02	0.05	0.07	-0.34	-1.46	-0.15	-0.55	-1.27	-0.05	-0.05	-1.27	-0.05	-0.34
Tip of the upper molar	-1.66	0.97	0.01	-0.01	0.19	-0.27	-1.45	-0.11	-0.51	-1.17	-0.25	-0.25	-1.17	-0.25	-0.3

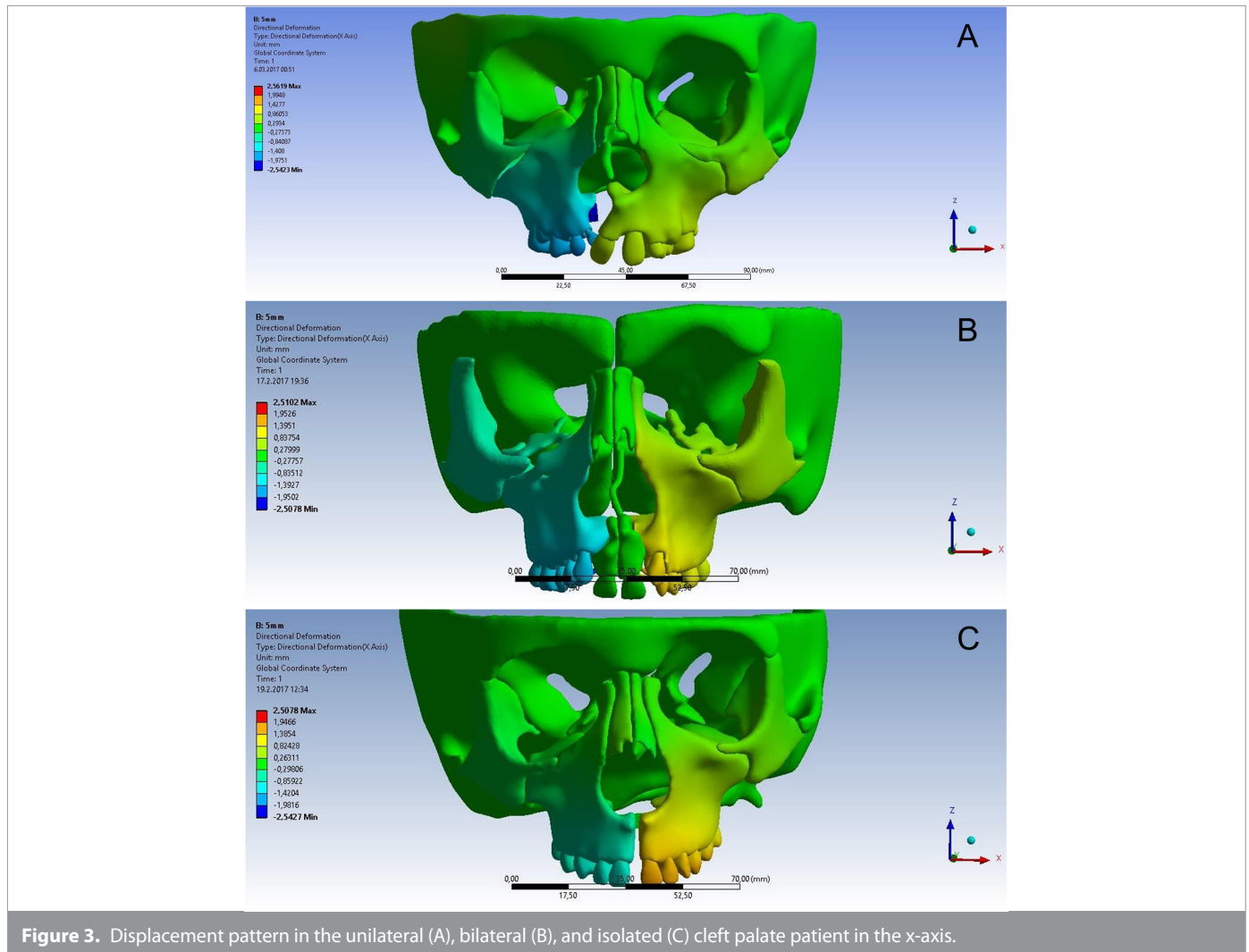


Figure 3. Displacement pattern in the unilateral (A), bilateral (B), and isolated (C) cleft palate patient in the x-axis.

other hand, the photoelastic models, which might be considered as an alternative experimental tool, have the disadvantage of exploring only the surface of the structures.¹⁰ Moreover, FEM is an accurate method that provides quantitative and detailed data regarding the responses occurring in the modeled tissues.¹¹

The reliability and accuracy of the FEM entirely depend on the validity of the model. The models developed in this study were based on DVT images. In our FEM studies, the material properties assigned to the elements were isotropic, homogeneous, and linearly elastic.^{7,9,12} We referred the material properties based upon average values used in former studies.^{7-9,13-15} Previous studies used shell elements for meshing the geometry.⁴ In this study, tetrahedral elements with 10 nodes were used for mesh generation because this element had a quadratic displacement behavior and was well suited to modeling irregular meshes.

Over the past years, simulation models of the craniofacial complex have improved with geometric precision. In 1994, Miyasaka-Hiraga et al.¹⁶ modeled the skull with 1776 single elements in an FEM study. Iseri et al.⁴ performed a study with a model that consisted of 2349 single elements in 1998. An increase in the geometric precision was observed in a study by Jafari et al.⁶ which

introduced a model with 6951 elements. Finally, in 2007, Holberg et al.¹⁷ used a simulation model that consisted of approximately 30 000 elements and 50 000 nodes. The finite element model of the craniofacial complex introduced here consisted of 2 785 413 elements and 1 799 565 nodes for the UCP model, 2 508 593 elements, and 1 609 498 nodes for the BCP model, 3 198 386 elements and 2 117 163 nodes for the ICP model.

According to the results of our study, the highest amount of transverse expansion was recorded for the BCP model. A similar amount of expansion has been observed in the cleft side of the UCP. Less expansion was recorded in the ICP model, followed by the non-cleft side of the UCP model. Mathew et al.¹⁸ compared different types of upper jaw expansion appliances, including hyrax and bone-borne palatal expander, in a UCP patient model, and found higher amounts of displacement on the cleft side with both appliances. That might be explained by the fact that the missing bone tissue in the cleft area causes less resistance to the expansion forces. However, clinically, a significant relapse tendency in cleft patients is associated with the scar tissue or soft tissue tension. Modeling soft tissue is very difficult in FEM studies, since it exhibits hyperelastic behavior. For this reason, soft tissues such as mimic muscles, chewing muscles, gingiva, soft

Table 3. Von Mises stress distribution of different cleft palate patients (MPa)

	Unilateral		Bilateral	Isolated
	Cleft Side	Non-cleft Side		
Sutura internasalis	19 360	19 360	0	46 447
Sutura frontonasalis	0.49	0.51	0	0.25
Sutura frontomaxillaris	32 143	0.72	0	0.19
Sutura nasomaxillaris	0.57	33 970	0	45 352
Sutura frontozygomatıca	0.53	0.14	0	0.06
Sutura temporozygomatıca	0	0	20 821	0
Sutura zygomatıcomaxillaris	16 650	19 725	33 635	1555
Infraorbital margin	23 833	0.56	0.42	1215
Foramen infraorbitalis	0.5	0.22	0.32	0.895
Zygomatıc process	0.5	0.57	0.53	23 774
Lateral nasal wall	0.76	0.73	0.38	43 466
ANS	-	0	-	0
Point A	-	0	-	0.035
Apical region of incisors	-	0.01	-	0.03
Apical region of canine	0.11	0.01	0.12	0.53
Apical region of premolars	0.42	0.17	0.17	0.69
Apical region of molars	0.34	0.21	0.07	44 044
Retromolar region	0.25	0.06	0.14	43 831
Tip of the upper central incisor	-	0	-	0
Tip of the upper canine	0	0	0	0
Tip of the upper premolar	0.89	46 023	0.34	0.83
Tip of the upper molar	0.18	0.17	0.35	1075

palate, velopharyngeal region, scar tissue, and the skin were not included in modeling. This is a major limitation in this and other FEM studies. In light of these, it might be assumed that fewer expansion forces are effective in UCP or BCP patients; however, the soft tissue reaction should be taken into consideration.

In response to the maxillary expansion procedure, the asymmetrical changes were also observed in other regions such as the zygomatic bone and the 2 halves of the maxilla. Consistent with our study results, previous studies have also documented asymmetric changes in UCP patients.^{2,19,20} Nicholson and Plint (1989),²¹ in Capelozza Filho et al. (1994),²² and later Pan et al.² mentioned a triangular opening with the base in the incisor teeth region and the apex in the nasal region, in accordance with our study.

Some authors concluded that the A point moves forward, others stated that it moves backward; contradictory to these 2 opposite findings, other researchers found that the A point's position remains stable following RME.^{5,23-27} According to the results of our study, A point moves backward in the UCP patient and moves forward in the ICP patient.

In a study by Wang et al.⁹ who evaluated the biomechanical outcomes of the RME in a UCP patient FEA model, most of the changes in the sagittal plane were found in the dental region,

indicating that these values gradually decreased from the inferior to the superior region. Similarly, the highest displacement values were found in the dental regions in all 3 CP models in our study; most of the anatomic structures in the UCP model tended to displace posteriorly, but the amount of displacement was asymmetric on the cleft and non-cleft sides. This asymmetric distribution is an expected condition due to the structural and functional asymmetry existing in anatomical structures of UCP patients. On the other hand, in the BCP model, all the structures tended to displace anteriorly. Interestingly, in the ICP model, the structures close to the midline tended to displace anteriorly, while lateral structures had the tendency for posterior displacement. This type of displacement has been previously reported in a clinical study by Yılmaz et al.²⁸ In light of these results, it might be assumed that fewer expansion forces might be effective in UCP or BCP patients. However, these findings should be interpreted with caution since the major limitation in the FEM studies is the lack of effects of the soft tissue, especially that of the palatal scar tissue in cleft patients. Even though the expansion procedure might be completed successfully with lesser forces, it should be kept in mind that there would be a greater relapse tendency.

Previous clinical studies reported that the maxilla displaces downward by Rapid Palatal Expansion (RPE). The clockwise rotation of the mandible after RPE was also reported in CLP patients.^{29,30} In our study, in the UCP and ICP models, the structures close to the

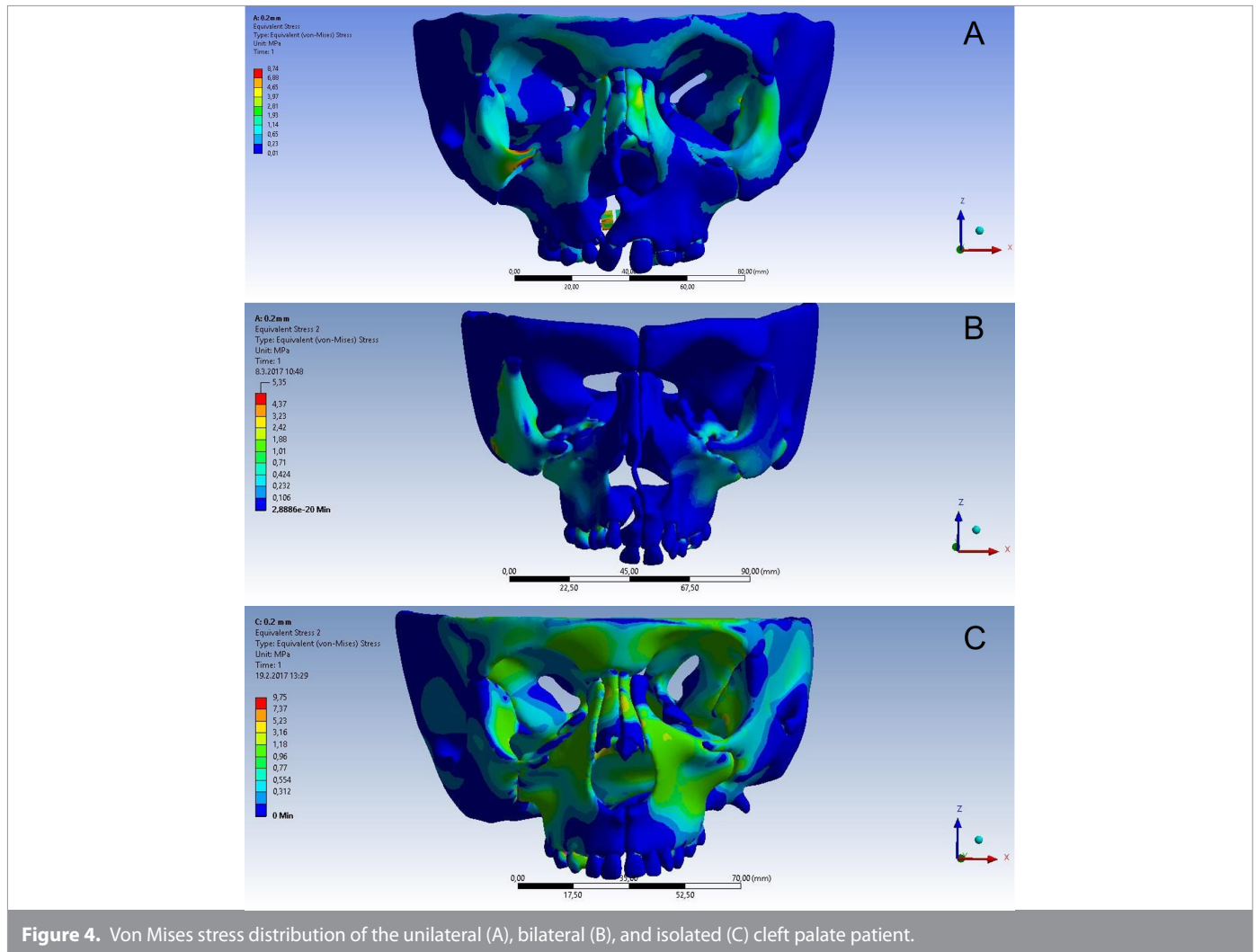


Figure 4. Von Mises stress distribution of the unilateral (A), bilateral (B), and isolated (C) cleft palate patient.

midline displaced downward, while the structures located more laterally showed upward displacement. In the BCP model, most of the anatomic structures showed a tendency toward inferior displacement. These findings are in harmony with those in the literature.^{9,29,30}

It is important to know whether there is a change in the mechanism of interaction between the expansion forces and the resistance areas in CP patients to be able to predict the treatment outcomes. Pan et al.² observed significant differences in skull models with and without a cleft. They reported that the stresses accumulated in the lateral buccal margin of the maxilla was greater than those previously reported in non-cleft patients. In our study, in the patient model with a unilateral cleft, relatively higher stress values were observed on the cleft side compared to the non-cleft side. The maximum von Mises stresses were found on the cleft side in the internasal, frontomaxillary, and zygomaticomaxillary suture areas, in harmony with the studies by Lee et al.³¹ and Gautam et al.⁵ On the other hand, in the model with bilateral cleft, maximum von Mises stresses were found in the zygomaticomaxillary and zygomaticotemporal suture areas, and no stress was recorded in any of the nasal landmarks. This difference in stress distribution might be related to the fact that

the stresses created by the expansive forces are directed to the lateral parts of the maxillary complex in BCP. In contrast, in UCP and ICP models, where the integrity of the alveolar bone is preserved, the stresses are also transferred to the internasal region.

In the present study, the greatest dental expansion among the 3 cleft models was observed in the BCP model, followed by the UCP model. In the UCP model, the amount of displacement and deformation was greater on the cleft side compared to that of the non-cleft side, indicating that asymmetric displacement and deformation occurs in UCP model following RPE. Based on these findings, it can be hypothesized that the RPE procedure should be customized to the patient's individual needs in cleft patients, depending the type of the cleft (primary or secondary palate), and the desired area of expansion (anterior or posterior).

CONCLUSION

- Different patterns of stress distribution occurred in response to expansion forces in all 3 different cleft type models. In the isolated cleft type, more stress accumulated especially in the nasal region. On the other hand, no stress was observed on landmarks in the nasal region for the bilateral cleft model.

- More intense stress accumulation was observed on the cleft side of the unilateral cleft model.
- The maximum dentoalveolar expansion in the cleft side of the unilateral, bilateral and isolated cleft patients occurred at the canine area, decreasing toward the posterior part. On the other hand, on the non-cleft side of the unilateral cleft model, the maximum dentoalveolar expansion occurred at the molar area, decreasing toward the anterior segment.
- In all 3 models, pyramidal opening occurred on the facial structures in the frontal plane.

Ethics Committee Approval: This study was approved by Ethics committee of Bezmialem Vakif University, Scientific Research Projects Commission. (Approval No:-6.2015/9).

Informed Consent: Written informed consent was obtained from the patients who agreed to take part in the study.

Peer Review: Externally peer-reviewed.

Author Contributions: Supervision – B.Y., S.I.R.; Design – E.B.; Concept – E.B., B.Y., S.I.R.; Resources – E.B.; Materials – E.B.; Data Collection and/or Processing – E.B., B.Y.; Analysis and/or Interpretation – E.B.; Literature Search – E.B., B.Y.; Writing Manuscript – E.B.; Critical Review – B.Y., S.I.R.

Acknowledgment: This study was based on the specialization thesis entitled ‘Stress distribution and displacement of craniofacial structures following rapid maxillary expansion in different types of cleft palate: a three-dimensional FEM study’ supported by Bezmialem Vakif University Scientific Research Projects Commission.

Conflict of Interest: The authors have no conflict of interest to declare.

Financial Disclosure: The authors declared that this study has received no financial support.

REFERENCES

1. Samuel Berkowitz NE. *Cleft Lip and Palate-Diagnosis and Management*. Berlin Heidelberg:Springer-Verlag; 2006. Mund-, Kiefer-und Gesichtschirurgie. 2007;11(1):59-60.
2. Pan X, Qian Y, Yu J et al. Biomechanical effects of rapid palatal expansion on the craniofacial skeleton with cleft palate: a three-dimensional finite element analysis. *Cleft Palate Craniofac J*. 2007;44(2):149-154. [CrossRef]
3. Capelozza Filho L, De Almeida AM, Ursi WJ. Rapid maxillary expansion in cleft lip and palate patients. *J Clin Orthod*. 1994;28(1):34-39.
4. Işeri H, Tekkaya AE, Öztan O, Bilgiç S. Biomechanical effects of rapid maxillary expansion on the craniofacial skeleton, studied by the finite element method. *Eur J Orthod*. 1998;20(4):347-356. [CrossRef]
5. Gautam P, Valiathan A, Adhikari R. Stress and displacement patterns in the craniofacial skeleton with rapid maxillary expansion: a finite element method study. *Am J Orthod Dentofac Orthop*. 2007;132(1):e1-5.11.
6. Jafari A, Shetty KS, Kumar M. Study of stress distribution and displacement of various craniofacial structures following application of transverse orthopedic forces—a three-dimensional FEM study. *Angle Orthod*. 2003;73(1):12-20. (doi:[CrossRef])
7. Tanne K, Hiraga J, Kakiuchi K, Yamagata Y, Sakuda M. Biomechanical effect of anteriorly directed extraoral forces on the craniofacial complex: a study using the finite element method. *Am J Orthod Dentofac Orthop*. 1989;95(3):200-207. [CrossRef]
8. Gupta A, Kohli VS, Hazarey PV, Kharbanda OP, Gunjal A. Stress distribution in the temporomandibular joint after mandibular protraction: a 3-dimensional finite element method study. Part 1. *Am J Orthod Dentofac Orthop*. 2009;135(6):737-748. [CrossRef]
9. Wang D, Cheng L, Wang C, Qian Y, Pan X. Biomechanical analysis of rapid maxillary expansion in the UCLP patient. *Med Eng Phys*. 2009;31(3):409-417. [CrossRef]
10. Knop L, Gandini LG Jr, Shintcovsk RL, Gandini MR. Scientific use of the finite element method in Orthodontics. *Dent Press J Orthod*. 2015;20(2):119-125. [CrossRef]
11. Kamble RH, Lohkare S, Hararey PV, Mundada RD. Stress distribution pattern in a root of maxillary central incisor having various root morphologies: a finite element study. *Angle Orthod*. 2012;82(5):799-805. [CrossRef]
12. Tanne K, Yoshida S, Kawata T et al. An evaluation of the biomechanical response of the tooth and periodontium to orthodontic forces in adolescent and adult subjects. *Br J Orthod*. 1998;25(2):109-115. [CrossRef]
13. Ludwig B, Baumgaertel S, Zorkun B et al. Application of a new viscoelastic finite element method model and analysis of miniscrew-supported hybrid hyrax treatment. *Am J Orthod Dentofac Orthop*. 2013;143(3):426-435. [CrossRef]
14. Hong HR, Pae A, Kim Y et al. Effect of implant position, angulation, and attachment height on peri-implant bone stress associated with mandibular two-implant overdentures: a finite element analysis. *Int J Oral Maxillofac Implants*. 2012;27(5):e69-e76.
15. Jeon PD, Turley PK, Moon HB, Ting K. Analysis of stress in the periodontium of the maxillary first molar with a three-dimensional finite element model. *Am J Orthod Dentofac Orthop*. 1999;115(3):267-274. [CrossRef]
16. Miyasaka-Hiraga J, Tanne K, Nakamura S. Finite element analysis for stresses in the craniofacial sutures produced by maxillary protraction forces applied at the upper canines. *Br J Orthod*. 1994;21(4):343-348. [CrossRef]
17. Holberg C, Steinhäuser S, Rudzki-Janson I. Rapid maxillary expansion in adults: cranial stress reduction depending on the extent of surgery. *Eur J Orthod*. 2007;29(1):31-36. [CrossRef]
18. Mathew A, Nagachandran KS, Vijayalakshmi D. Stress and displacement pattern evaluation using two different palatal expanders in unilateral cleft lip and palate: a three-dimensional finite element analysis. *Prog Orthod*. 2016;17(1):38. [CrossRef]
19. Holberg C, Holberg N, Schwenzler K, Wichelhaus A, Rudzki-Janson I. Biomechanical analysis of maxillary expansion in CLP patients. *Angle Orthod*. 2007;77(2):280-287. [CrossRef]
20. Isaacson RJ, Ingram AH. Forces produced by rapid maxillary expansion: II. Forces present during treatment. *Angle Orthod*. 1964;34(4):261-270.
21. Nicholson PT, Plint DA. A long-term study of rapid maxillary expansion and bone grafting in cleft lip and palate patients. *Eur J Orthod*. 1989;11(2):186-192. [CrossRef]
22. Capelozza Filho L, De Almeida AMd, Ursi WJdS. Rapid maxillary expansion in cleft lip and palate patients. *J Clin Orthod*. 1994;28(1):34-39.
23. Basciftci FA, Karaman AI. Effects of a modified acrylic bonded rapid maxillary expansion appliance and vertical chin cap on dentofacial structures. *Angle Orthod*. 2002;72(1):61-71. [CrossRef]
24. Sari Z, Uysal T, Usumez S, Basciftci FA. Rapid maxillary expansion. Is it better in the mixed or in the permanent dentition? *Angle Orthod*. 2003;73(6):654-661. [CrossRef]
25. Sarver DM, Johnston MW. Skeletal changes in vertical and anterior displacement of the maxilla with bonded rapid palatal expansion appliances. *Am J Orthod Dentofac Orthop*. 1989;95(6):462-466. [CrossRef]

26. de Silva OG, Boas CV, Capelozza LF. Rapid maxillary expansion in the primary and mixed dentitions: a cephalometric evaluation. *Am J Orthod Dentofac Orthop.* 1991;100(2):171-179.
27. Reed N, Ghosh J, Nanda RS. Comparison of treatment outcomes with banded and bonded RPE appliances. *Am J Orthod Dentofacial Orthop.* 1999;116(1):31-40. [\[CrossRef\]](#)
28. Yilmaz BS, Kucukkeles N. Skeletal, soft tissue, and airway changes following the alternate maxillary expansions and constrictions protocol. *Angle Orthod.* 2014;85(1):117-126.
29. Isaacson RJ, Murphy TD. Some Effects of rapid maxillary expansion in cleft lip and palate patients. *Angle Orthod.* 1964;34(3):143-154.
30. Tindlund RS, Rygh P, Bøe OE. Intercanine widening and sagittal effect of maxillary transverse expansion in patients with cleft lip and palate during the deciduous and mixed dentitions. *Cleft Palate Craniofac J.* 1993;30(2):195-207. [\[CrossRef\]](#)
31. Lee H, Nguyen A, Hong C et al. Biomechanical effects of maxillary expansion on a patient with cleft palate: a finite element analysis. *Am J Orthod Dentofacial Orthop.* 2016;150(2):313-323. [\[CrossRef\]](#)